ELSEVIER

Biochimica et Biophysica Acta 1468 (2000) 239–252

BIOCHIMICA ET BIOPHYSICA ACTA
BBA

www.elsevier.com/locate/bba

Efficient encapsulation of DNA plasmids in small neutral liposomes induced by ethanol and calcium

Austin L. Bailey *, Sean M. Sullivan

Valentis, Inc., 8301 New Trails Drive, The Woodlands, TX 77381-4248, USA

Received 10 April 2000; received in revised form 5 June 2000; accepted 8 June 2000

Abstract

Efficient encapsulation of DNA plasmids inside small, neutral liposomes composed of 1,2-dioleoyl-*sn*-phosphatidylcholine (DOPC), DOPC/DOPE (1,2-dioleoyl-*sn*-phosphatidylethanolamine) (1:1) and DOPC/DOPE/cholesterol (1:1:1) was achieved by the addition of ethanol and calcium chloride to an aqueous mixture of small unilamellar vesicles (SUVs) and plasmid. Following dialysis against low-salt buffer, the neutral lipid complexes (NLCs) had average effective diameters less than 200 nm and encapsulated up to 80% of the DNA. Optimum Ca^{2+} and ethanol concentrations for each lipid mixture were determined by statistically designed experiments and mathematical modeling of trapping efficiency. NLCs are unilamellar, have neutral surface potentials, and retain entrapped DNA at pH 4.0 and in serum at 37°C. The circulation and clearance properties of the complexes following intravenous administration in mice are similar to empty neutral liposomes, and the toxicity of NLCs are expected to be significantly reduced compared to other non-viral gene-delivery systems. The NLC encapsulation method, if it can be combined with effective targeting and endosome-release technologies to achieve efficient and tissue-specific transfection, may represent an important alternative to current systemic gene therapy approaches.

Keywords: DNA condensation; Lipid; Fusion; Gene therapy; Non-viral delivery system; Statistical experimental design

1. Introduction

Systemic gene delivery using DNA plasmids complexed with lipid vesicles or synthetic polymers offers an attractive alternative to recombinant viral vectors for gene therapy, with the advantages of lower costs of production and fewer safety concerns. While in vivo transfection with existing cationic delivery systems can be achieved by local administration, e.g. intratumoral injection, their charge properties and physical characteristics limit their efficacy in systemic applications. Specifically, the particles interact strongly with serum proteins, often leading to disassembly or clearance of the complexes before they can reach target tissues. Positively charged cationic liposome–plasmid complexes can passively target the lungs when administered intravenously [1]. However, the doses required for transfection of lung tissue using these complexes can be accompanied by vascular leakage, resulting in a narrow therapeutic window. Additionally, a strong cytokine response is associated with lung transfection, which may be undesirable for some applications [2]. Strategies to re-target cationic

* Corresponding author. Present address: ValiGen, Inc., 300 Pheasant Run, Newtown, PA 18940, USA.
Fax. +1-215-504-4545; E-mail: abailey@kimeragen.com

0005-2736/00/$ – see front matter
PII: S0005-2736(00)00264-9

lipid–DNA complexes to other tissues and to reduce lung-associated toxicity have met with some success (for a review, see [3]).

Liposomes composed of neutral or zwitterionic lipids have much longer circulation times, lower toxicities, and very different clearance profiles compared to cationic particles. Neutral liposomes have been successfully applied as carriers for anti-cancer drugs and antibiotics, to achieve lower toxicities, altered distributions, and higher drug efficacies than unencapsulated drugs (for reviews, [4–6]). Small, neutral liposomes passively accumulate in tumors and sites of inflammation where the vasculature is malformed or permeabilized [7]. In addition, re-targeting strategies are more easily applied to neutral liposomes than to cationic complexes, given their increased circulation lifetimes. In terms of systemic delivery of plasmids, however, neutral liposomes have two distinct disadvantages relative to cationic liposomes: a lack of capacity to achieve any appreciable level of transfection, and no existing methods for efficient entrapment of DNA plasmids in particles of sufficiently small size for systemic administration. The problem of transfection is currently being addressed by the use of pH-sensitive, membrane-lytic peptides and polymers that can be grafted to liposomes to deliver liposomal contents to the cytosol following endocytosis. In this paper, we present a method to efficiently trap plasmids inside small neutral liposomes.

The encapsulation of DNA plasmids in liposomes has been achieved by a number of techniques with varying degrees of success. The reverse-phase evaporation method [8] produces large unilamellar liposomes (average diameters of 400–500 nm) in which up to 40% of plasmids can be trapped using negatively charged, phosphatidylserine (PS)-containing vesicles [9,10]. Dehydration–rehydration techniques [11,12] have also been adapted with claims of greater than 60% plasmid entrapment in oleic acid-containing vesicles, but most of the entrapped plasmid is released by extrusion through 0.45-μm filters [13], suggesting that the vesicles are very large. Smaller vesicles prepared by a detergent dialysis method, again with oleic acid in the lipid mixture, gave 15% trapping in 200-nm liposomes [14]. A more obscure method of entrapment by the addition of EDTA to Ca^{2+}-PS cochleates in the presence of DNA has been shown to be far less efficient, with less than 1% trapping achieved [15].

It is not straightforward to compare results from these studies, since different mixtures of lipids and variations in procedures can greatly influence trapping efficiencies. In many cases, charged lipids have been used, either to enhance plasmid interactions or to increase transfection in vitro. However, both the membrane charge and the large particle sizes of these preparations can be detrimental to in vivo delivery. A direct comparison of three different encapsulation techniques using the zwitterionic lipid POPC (1-palmitoyl-2-oleoyl-*sn*-phosphatidylcholine) showed that a freeze–thaw procedure [16] was superior (30% plasmid entrapped) to both the dehydration–rehydration (14%) and the reverse-phase (11%) methods for entrapment in liposomes with average diameters less than 200 nm [17]. In this study, plasmid entrapment was enhanced by the addition of cationic lipids, but inhibited in the presence of normal saline.

Given that the optimal liposome size for extended circulation is 100–200 nm, the limiting factors in achieving higher entrapment of plasmids in neutral liposomes are: the relative size of the plasmid, with average radii of gyration on the scale of 80–125 nm depending on the sequence length and the supercoil–open circle ratio [18]; and the low passive entrapment volume for liposomes of this size. For example, 150-nm unilamellar liposomes at a lipid concentration of 10 mM contain only 3–5% of the total aqueous volume in which they are suspended. To overcome these disadvantages, methods that either condense the plasmid, or increase lipid–DNA interactions, or both, are needed to increase the probability of plasmid entrapment.

The condensation of DNA by divalent metal ions has been extensively studied. The transition metal ions Mn^{2+}, Ni^{2+}, Co^{2+}, and Cu^{2+} have all been shown to condense DNA through neutralization of the phosphate groups of the DNA backbone and distortion of the B-DNA structure through hydrogen bonding with bases, permitting both local bending of the DNA and inter-helical associations [19–22]. The concentrations of metal ions required for such condensation are known to be dependent on the dielectric constant of the medium [23]. The addition of ethanol or methanol greatly reduces the concentration of metal ion required [24]. Ethanol itself can also

be used for controlled condensation of DNA at concentrations up to 60% by volume [25–27].

Calcium ions will also condense DNA, albeit at higher concentrations than required for the transition metal ions [28]. Recently, it has been shown that Ca^{2+} not only binds to DNA phosphates, but can also form a complex with the nitrogen$_{(7)}$ and oxygen$_{(6)}$ of guanine, disrupting base pairing [22]. The potential advantages of using calcium for plasmid condensation are: its lower binding affinity for DNA, making the condensation more easily reversed by the removal of calcium or the competitive binding of high concentrations of Na^+; the wider concentration ranges over which condensation occurs, giving greater control over this highly co-operative process; and reduced potential toxicity owing to tight cellular regulation of calcium.

Interestingly, calcium has also been shown to be capable of mediating the binding of DNA to small unilamellar vesicles (SUVs) composed of phosphatidylcholine (PC) and the encapsulation of DNA inside large POPC unilamellar vesicles (LUVs) prepared by the reverse phase method described above [29–31]. Uptake of up to 15% of a sonicated T7 phage DNA was achieved, reportedly by a mechanism involving invagination and pinching off of smaller vesicles within the larger liposomes. Similar results have since been reported by others using multi-lamellar vesicles (MLVs) [32] or extruded vesicles [33] of PC, although the structures of the resulting complexes were less well characterized in the latter studies.

Given these reports of PC liposome entrapment of DNA, and the stability and increased circulation properties of PC bilayers relative to cationic liposomes, we chose pure DOPC liposomes for our initial attempts to entrap plasmids using combinations of calcium and ethanol. DOPC, with two mono-unsaturated acyl chains, is liquid-crystalline at ambient and physiological temperatures and forms more stable SUVs than the pure, saturated phosphatidylcholines with comparable hydrocarbon chain lengths [34]. However, DOPC has a higher propensity to support membrane fusion relative to monounsaturated lipids, e.g. POPC [35], a property that is desirable for the eventual release of entrapped DNA. The propensity of DOPC bilayers to fuse with other membranes can be increased by the addition of 1,2-dioleoyl-*sn*-phosphatidylethanolamine (DOPE), a fusogenic zwitterionic lipid. Cholesterol, while reducing membrane permeability of PC membranes, can also promote fusion as a result of its curvature-inducing properties [36]. For these reasons, we have also studied plasmid entrapment in DOPC/DOPE (1:1) and DOPC/DOPE/Chol (1:1:1) mixtures, all of which are charge-neutral.

We describe a method for trapping DNA plasmids inside unilamellar liposomes with average diameters less than 200 nm and trapping efficiencies up to 80%. Entrapment is induced by the simultaneous addition of calcium and ethanol, followed by dialysis against low-salt buffer. Optimized conditions for each of the three lipid mixtures are determined. In addition to size and entrapment analysis of the resulting neutral lipid complexes (NLCs), the lamellarity, the in vitro stability, and the biodistribution following intravenous administration are reported.

2. Materials and methods

2.1. Materials

The phospholipids, 1,2-dioleoyl-*sn*-phosphatidylcholine (DOPC) and 1,2-dioleoyl-*sn*-phosphatidylethanolamine (DOPE), cholesterol, and head-group labeled NBD-DOPE were purchased as chloroform solutions from Avanti Polar Lipids (Alabaster, AL). Tritium-labeled cholesteryl hexadecyl ether was supplied by NEN (Boston, MA). Absolute ethanol was from Millennium Petrochemicals (Tuscola, IL), and calcium chloride and sodium dithionite were purchased from Sigma (St. Louis, MO). TO-PRO-1, Indo-1, and Cyber Green were supplied by Molecular Probes (Eugene, OR). Concentrated Tris–HCl, pH 8.0, and phosphate buffered saline, pH 7.4 (PBS), were from Gibco-BRL (Rockville, MD). Regenerated cellulose dialysis tubing (3500 MWCO) and pre-sterilized dialysis tubes (10 000 MWCO) were supplied by Spectra/Por.

2.2. Liposome preparation

Chloroform solutions of lipids were mixed and dried to a thin film by rotary evaporation. Residual solvent was removed under high vacuum for at least

4 h or overnight. Dried lipids were dispersed with 10 mM Tris buffer, pH 7.4 (TB7.4), to a concentration of 80 mM total lipid in volumes ranging from 1 to 5 ml. Small unilamellar vesicles (SUVs) were formed by probe sonication (Fisher Scientific). A sonication program (five cycles of 3-min pulsing, 1-min off) and immersion of the sample tube in an ice bath throughout the process were used to minimize sample heating. Liposomes were then centrifuged at 12 000 rpm in an Eppendorf 5415C centrifuge for 5 min to remove debris, and filtered through 0.2-μm sterilizing membranes.

2.3. Plasmid preparation

Plasmid (pCMV-CAT, 4377 bp) was isolated and purified from *Escherichia coli* as described previously [37]. The purity of plasmid preparations was determined by 1% agarose gel electrophoresis followed by SYBR Green fluorescent staining. DNA concentration was measured by UV absorption at 260 nm. The percentage of supercoiled pDNA was in the range of 80–95%, and the $OD_{260/280}$ ratio was between 1.85 and 1.9. Endotoxin levels of pDNA were determined using a chromogenic limulus amebocyte lysate assay (LAL BioWhitaker, Walkersville, MD). Values were less than 20 EU/mg.

2.4. Formation and optimization of NLCs

Neutral liposome complexes (NLCs) were formed by first mixing SUVs (250 μl, 20 μmol), plasmid (0.1 mg), and TB7.4 to give a total volume of 400 μl. To this was added 600 μl of a given mixture of absolute ethanol, calcium chloride (from a 500 mM stock) and TB7.4. Addition was drop-wise over approximately 30 s with maximum vortex mixing. The resulting aggregated complexes were dialyzed against 500 vols. of TB7.4 for 24 h with two changes of buffer. For experiments requiring physiological tonicity, samples were further dialyzed against 500 vols. of PBS for 24 h.

For a given lipid composition, plasmid entrapment and particle size were optimized using central composite experimental designs with two factors (ethanol and calcium concentrations) and four centerpoints. Design and analysis were performed using Essential Experiment Design, an add-in macro for Microsoft Excel [38]. Factor ranges were estimated from preliminary trapping experiments, and these were different for each lipid composition: DOPC, 35–50% ethanol, 0–5 mM Ca^{2+}; DOPC/DOPE, 20–40% ethanol, 0–10 mM Ca^{2+}; DOPC/DOPE/Chol, 35–45% ethanol, 5–15 mM Ca^{2+}. Quadratic models with up to six terms were fit to the measured entrapment data from each design, but only those terms that contributed significantly to the fit ($P < 0.05$) were used in predicting optimal formulations. The criteria for optimization were maximized entrapment and average particle size less than 200 nm. A single design was required to optimize each lipid formulation, but each was repeated to validate the resulting model and terms.

2.5. Size analysis

Average particle diameters were determined by quasi-elastic light scattering (QELS) using a BI-9000AT correlator (Brookhaven Instruments, Holtsville, NY). Samples were diluted to 1.0 mM lipid in water or PBS, as appropriate, to give sufficient scattering intensity with a minimum pinhole (100 μm). Averages of three autocorrelations, each collected over 1 min with a minimum scattering intensity of 5×10^4 counts/s, were converted to Gaussian distributions, from which mean diameters and standard deviations were derived using software supplied by the manufacturer. Polydispersities were also noted.

2.6. Entrapment assay

The fraction of plasmid entrapped by the complexation procedure was determined using the fluorescent DNA probe TO-PRO-1 [39]. Complexes were diluted 100-fold into a total 2.0 ml volume with TB7.4, and 1 μl of 1 mM TO-PRO-1 was added from a DMSO stock solution. Fluorescence was measured on a Perkin-Elmer LS 50B spectrofluorometer, with excitation and emission wavelengths of 514 and 531 nm, respectively, 2.5 nm slit-widths, and the photo-multiplier voltage set to 900 V. The signal due to scatter prior to the addition of TO-PRO-1 was set to zero fluorescence. Percent entrapment was calculated as the fluorescence signal of TO-PRO-1 divided by the fluorescence following the addition of 20 μl of 100 mM Triton X-100 to release DNA from the lipid,

correcting for the 1% increase in volume. At the concentrations specified, the neutral lipids and Triton X-100 were determined to have no effect on TO-PRO-1 fluorescence in the presence of free DNA plasmids. Increasing the concentration of TO-PRO-1 did not increase fluorescence, indicating that it is present in sufficient excess.

2.7. Negative stain electron microscopy

Just prior to use, formar-coated 100-mesh copper grids were prepared by glow discharging. Grids were then floated on 25 μl of sample for 90 s, wicked off, and floated on drops of 1% aqueous uranyl acetate for 90 s. Finally, samples were wicked off, air dried and stored at room temperature. Negative stain electron micrographs of NLCs were taken using a JEOL 1200EX electron microscope, operating at 60 kV. Images were recorded at a magnification of 100 000×.

2.8. Zeta potential and lamellarity

Surface charges of SUVs and NLCs were measured on a Malvern Zetasizer 2000 using a dip cell and disposable polyacrylate cuvettes. Samples were diluted to 0.2 mM lipid in TB7.4 to achieve sufficient signal with scatter less than 1.5×10^5 counts per second. Measurements were made using the automated procedure provided with the instrument.

Lamellarity of NLCs was measured by a procedure adapted from Gruber and Schindler [40]. Complexes with a final average diameter of approximately 150 nm were made from DOPC SUVs containing 0.1 mol% NBD-DOPE using the entrapment procedure described above. Twenty microliters of NLCs or 5 μl of SUVs were diluted to 2 ml in TB7.4 or PBS, as appropriate, and fluorescence was monitored at 540 nm with excitation at 470 nm and 5 nm slit-widths. After 2 min, 20 μl of a freshly prepared sodium dithionite solution (prepared by mixing 348 mg $Na_2S_2O_4$ and 243 mg of Tris free base in 1.55 ml of water) was added. Four minutes later, 20 μl of 100 mM Triton X-100 was added to disrupt liposomes and allow complete bleaching of the probe. An experiment in which Triton X-100 was added before dithionite was used to control for scatter by the relatively large complexes in the absence of a low-pass filter. Lamellarity was calculated as described in Fig. 3.

2.9. Stability assays

Ten milliliters of DOPC or DOPC/DOPE (1:1) NLCs, prepared at optimized conditions, were concentrated to 1.0 ml (1.0 mg/ml DNA) in two Ultrafree-15 Biomax 100 kDa nominal molecular weight cut-off centrifugal filters (Millipore, Bedford, MA) by spinning at $2500\times g$ for 30 min in a bench-top centrifuge. Concentrated complexes were stored for 14 days at 4°C, or diluted 10-fold into either PBS, pH 4.0, or fetal bovine serum (Gibco-BRL, Rockville, MD) and incubated at 37°C for 1 h. Particle size and entrapment of appropriately diluted complexes were measured as described above.

2.10. In vivo distribution

Subcutaneous solid tumors were created in the flanks of 6–8-week-old female C3H mice (20–22 g) (Charles River Laboratories, Raleigh, NC) by s.c. injection of 4×10^5 squamous carcinoma cells [41] 7 days prior to the experiment. For in vivo lipid distributions, DOPC SUVs, radiolabeled with a trace amount of the non-exchangeable lipid marker ^{3}H-cholesteryl hexadecyl ether (840 cpm/μl), were prepared by extrusion through 50 nm pore-size polycarbonate filters (Millipore), using a LiposoFast extruder (Avestin, Ottawa, ON). NLCs were formed using optimized conditions for DOPC, followed by concentration to 0.25 mg/ml DNA. Groups of five mice were tail-vein injected with either 300 μl of NLCs or 300 μl or an equivalent lipid dose of SUVs without DNA. One hour after injection, blood, tumors, livers, spleens, and lungs were harvested. Livers were homogenized in four parts water by Polytron. Two hundred microliters of liver homogenate, 100 μl blood, and other whole organs were digested in 5 ml scintillation vials by the addition of 50 μl 200 mM EDTA, 150 μl 30% hydrogen peroxide, and 25 μl 10 M HCl and incubating overnight at 50°C. After the addition of 4.5 ml of ScintiSafe 50% scintillation cocktail (Fisher Scientific, Springfield, NJ) and a further 24 h incubation at room temperature, radioactivity of the samples was measured using 5-min tritium counts on a Beckman LS6000SC.

Background counts were determined from organs harvested from uninjected mice.

In vivo distribution of plasmid was determined after tail-vein administration of 300 μl (90 μg DNA) unlabelled DOPC NLCs. Blood and organs were digested by incubation in 100 mM NaCl, 10 mM Tris–HCl, pH 8.0, 25 mM EDTA, pH 8.0, 0.5% SDS, and proteinase K, 0.1 mg/ml, at 50°C. The samples were extracted with an equal volume of Tris-buffered phenol, followed by extraction with chloroform/isoamyl alcohol (24:1, v/v) and ethanol precipitation. The DNA precipitates were dissolved in 10 mM Tris, pH 7.5, 1 mM EDTA, and DNA concentration was measured by UV absorption at 260 nm. CAT plasmid was quantified by polymerase chain reaction (PCR) using Taqman PCR (Perkin-Elmer, Foster City, CA). The primers used in the reaction were a forward primer, 5′-TGA CCT CCA TAG AAG ACA CCG GGA C-3′ (Genosys Biotechnologies, The Woodlands, TX), which primes in the CMV 5′-untranslated region (UTR), and a reverse primer, 5′-GCA AGT CGA CCT ATA ATG CCG-3′, which primes in the CAT coding region. The probe sequence was 5′-CCA GCC TCC GGA CTC TAG AGG A-3′. The initial copy numbers of unknown samples were determined by using an Applied Biosystem 7700 sequence detector to compare them with a standard curve generated from purified pCMV-CAT of known initial copy numbers.

3. Results

The size of SUVs produced by the sonication procedure was dependent on lipid composition. DOPC gave the smallest vesicles with mean diameters ranging from 35 to 45 nm, and polydispersity indices (P.I.) between 0.1 and 0.2. DOPC/DOPE (1:1) were larger (70–80 nm), but more monodisperse (P.I. = 0.08), due to the lower spontaneous curvature of this lipid mixture and the tendency of small vesicles to fuse spontaneously. Smaller DOPC/DOPE (1:1) populations could be produced by extrusion, but these spontaneously fused to larger sizes within hours in the low-salt buffer. The DOPC/DOPE/Chol (1:1:1) mixture could not produce vesicles smaller than 100 nm in diameter, even after doubling the sonication time or extrusion through 50-nm pore-size filters. To minimize spontaneous fusion of all SUVs prior to complexation with DNA, NLCs were prepared on the day of the sonication procedure.

Initial attempts to achieve entrapment of plasmids in liposomes by the addition of ethanol, calcium, or both ethanol and calcium were unsuccessful. Most procedures tried either resulted in very large particles or negligible entrapment of plasmid. Addition of ethanol alone to SUV-plasmid mixtures gave high entrapment of plasmid only with very large particle sizes. Ca^{2+} in the range of 2–20 mM was found to limit the sizes of these complexes. However, the trapping efficiency was sensitive to small changes in the calcium concentration, decreasing with increasing calcium.

Attempts to 'pre-condense' the plasmid with ethanol and calcium before the addition of liposomes or to destabilize liposomes by adding ethanol before the addition of plasmid were also ineffective. It became evident that condensation of the plasmid and aggregation and fusion of the liposomes needed to occur simultaneously in the mixture. Under these conditions, the plasmid interactions with, and entrapment in, fusing liposomes probably competes with condensation and aggregation of the plasmid. The liposome and plasmid concentrations are crucial parameters. For 100 μg/ml DNA, 20 mM lipid was required to achieve sub-micron particle sizes. These concentrations were used throughout the study. Assuming unilamellar liposomes with an average final diameter of 150 nm, this ratio is equivalent to approximately one plasmid for every two liposomes.

Physiological saline was found to prevent entrapment of plasmid completely under all conditions tried, even when very large lipid structures were formed. The salt may act to compete with calcium for binding to plasmid, thereby preventing condensation, and it may shield surface charges and prevent calcium-bridged lipid–DNA interactions.

Since the nature of these interactions and the mechanism of entrapment is unknown, we chose to explore a range of ethanol and calcium ion concentrations to determine conditions that give maximum entrapment of plasmid in particles less than 200 nm in diameter. Statistically designed experiments provide a convenient means to study the effects of simul-

taneously varying ethanol and calcium ion concentrations, without making any assumptions about their individual and correlated effects on entrapment and particle size. Extensive iterative titrations of each of the components to find an optimal formulation can be avoided.

We chose a central composite design with four centerpoints, which for two variables results in 12 experiments per design. Ranges of ethanol and calcium ion concentrations were chosen based on preliminary experiments showing entrapment, and these ranges are given in the methods. An example of such a design, using DOPC/DOPE (1:1) SUVs, is given in Table 1. Experiments were randomized within each design. For each experiment, effective diameters of particles and percent plasmid entrapment were determined and entered into the analysis. The reproducibility of the procedure is evident from the centerpoint repeats.

Quadratic models of increasing complexity were used to fit the trapping efficiency or the particle size. The number of significant terms required to achieve a fit varied with the lipid composition. In the example shown, the resulting equation that best describes the entrapment efficiency ($R^2 = 0.95$) was:

$$\%\ \text{Entrapment} = 94.0 + 2790 * \text{EtOH}^2 - 1100 * \text{EtOH} + 12.9 * [Ca^{2+}] - 41.8 * \text{EtOH} * [Ca^{2+}]$$

where EtOH is the fractional volume of ethanol and the calcium concentration is given in millimolar units. A comparison of plasmid entrapment predicted by this model with the experimental data is shown in Fig. 1. The raw data is also plotted to show that trapping efficiency increases sharply over a relatively narrow range of particle diameters, 120–160 nm.

In a similar modeling procedure for the formation of DOPC NLCs, only the square of the ethanol concentration and an inverse linear calcium term were required for a highly significant fit to observed trapping efficiency ($R^2 = 0.99$):

$$\%\ \text{Entrapment} = -51.2 + 532 * \text{EtOH}^2 - 2.5 * [Ca^{2+}]$$

With DOPC/DOPE/Chol (1:1:1) the best fit was

Table 1
Partial output from Essential Experimental Design for optimization of entrapment with DOPC/DOPE (1:1) liposomes and pCMV-CAT plasmid, 20–40% ethanol (v/v), 0–10 mM Ca^{2+}

Experiment[a]	EtOH (v/v)	Ca^{2+} (mM)	Size (nm)	% Entrapment
1	0.300	5.00	113.7	14.29[b]
2	0.300	5.00	111.9	15.70[b]
3	0.229	8.54	116.7	15.49
4	0.300	0.00	86.3	0.33
5	0.371	8.54	117.8	42.07
6	0.371	1.46	262.5	69.55
7	0.200	5.00	118.1	−0.06
8	0.300	5.00	110.9	13.83[b]
9	0.229	1.46	116.7	1.14
10	0.400	5.00	159.4	75.37
11	0.300	5.00	110.4	14.66[b]
12	0.300	10.00	105.5	16.23
Term	Coefficient[c]	*P* value	Standard error	
Intercept	9.40E+01	1.20E−01	5.31E+01	
EtOH × EtOH	2.79E+03	1.38E−03	5.46E+02	
EtOH	−1.11E+03	1.32E−02	3.37E+02	
Ca^{2+}	1.29E+01	1.99E−02	4.29E+00	
EtOH × Ca^{2+}	−4.18E+01	2.09E−02	1.41E+01	

[a]The 12 experiments from the central composite design were randomized.
[b]Four centerpoint repeats.
[c]Optimized values for the intercept and the co-efficients from a quadratic model, including all statistically significant terms (i.e. $P < 0.05$) along with their standard errors.

given by the same four-term model as for DOPC/DOPE (1:1), ($R^2 = 0.92$):

$$\% \text{ Entrapment} = -102 - 1538 * \text{EtOH}^2 + 901 * \text{EtOH} - 3.7 * [\text{Ca}^{2+}] + 12.8 * \text{EtOH} * [\text{Ca}^{2+}].$$

The equations of best fit are purely empirical and the co-efficients may not have deducible physical significance or any validity or outside of the factor ranges used. The fits were simply used to choose optimal formulations within the experimental ranges. More important conclusions might be drawn from the relative significance of each of the terms in the fit. For all three lipid mixtures, the trapping efficiency is primarily a function of the square of the ethanol concentration, with P values ranging from $< 10^{-9}$ for DOPC up to 0.0014 for DOPC/DOPE (1:1).

Analysis of the particle diameter data following identical modeling procedures shows that the effective diameter of the NLCs closely parallels trapping efficiency, except that higher calcium concentrations play a significant role in reducing particle size for a given trapping efficiency. Therefore, we chose conditions that maximized percent entrapped DNA, but that also produced NLCs for which the majority of particles would have effective diameters less than 200 nm (i.e. mean+S.D. ≤ 200 nm). The optimal conditions for each of the lipid mixtures studied are given in Table 2.

For DOPC and DOPC/DOPE (1:1) the optimization procedure was successful. Trapping efficiencies from 65–80% were achieved with average particle sizes 140 and 160 nm, respectively. Lower ethanol concentrations were required for the DOPE-containing liposomes, owing to their relative instability and propensity to fuse. However, higher calcium ion concentrations were also required, indicating that calcium plays a role either directly, or indirectly through plasmid effects, in limiting the extent of liposome fusion during NLC formation. It should be noted that the reduction in size achieved at higher calcium concentrations is not simply an osmotic effect on the

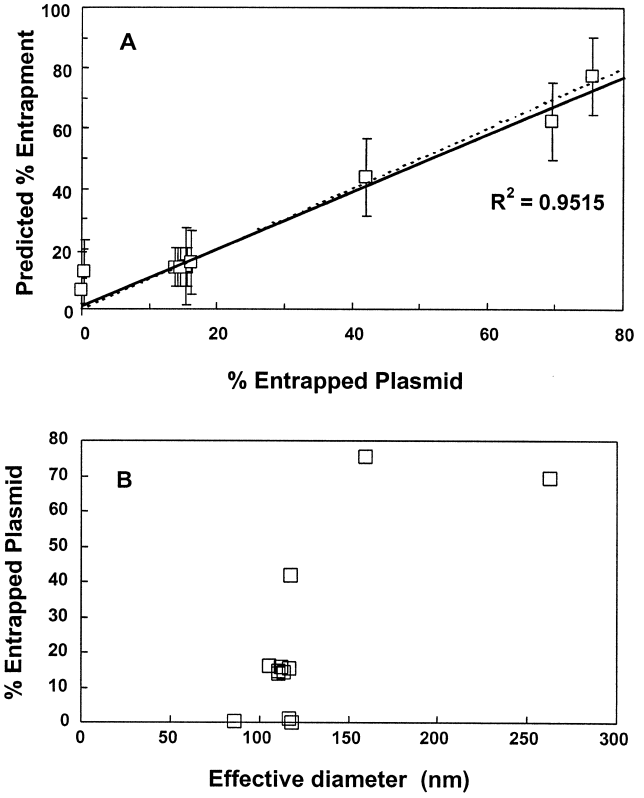

Fig. 1. Graphical output from Essential Experimental Design for optimization of entrapment with DOPC/DOPE (1:1) liposomes and pCMV-CAT plasmid, 20–40% ethanol (v/v), 0–10 mM Ca^{2+}. (A) Correlation curve from the quadratic model defined in Table 1, showing the level of fit to the experimental data for entrapment. The line represents the model of best fit with five terms. The error bars represent 95% confidence intervals on predicted values. The solid line is a least squares fit showing minimal deviation from slope = 1 (dotted line). (B) Raw data from the 12 experiments in the design plotted as % entrapped DNA vs. average effective particle diameter.

Table 2
Concentrations of ethanol and Ca^{2+} for optimized plasmid entrapment with three liposome compositions

Lipid composition	Optimized formulation	Effective diameter (nm)	% Entrapment[a]
DOPC	47.5% EtOH 4 mM Ca^{2+}	140 (30)[b]	65–70
DOPC/DOPE (1:1)	38% EtOH 8 mM Ca^{2+}	160 (40)	70–80
DOPC/DOPE/Chol (1:1:1)	38% EtOH 10 mM Ca^{2+}	>200	35–40

[a]Ranges are approximated from results from several independent designs.
[b]Standard deviations are in brackets.

complexes, since sizes are determined following removal of the calcium by dialysis.

In the case of DOPC/DOPE/Chol (1:1:1), it was not possible to achieve small particles with high plasmid entrapment. The best conditions gave 30–40% trapping efficiency with particle sizes between 200 and 400 nm. The inability to form SUVs from these lipids with diameters less than 100 nm, either by extended sonication or extrusion, likely contributes to the large size of the complexes. During NLC formation, it may be that the highly unstable nature of lipid bilayers composed of this mixture leads to a higher rate of liposome–liposome fusion events such that plasmid interactions are pre-empted. Perhaps the number of liposome–plasmid interactions is simply reduced in the presence of cholesterol. Because of the undesirably large size of these complexes, further characterization of the NLCs was limited to the DOPC and DOPC/DOPE (1:1) systems.

Removal of ethanol and calcium by dialysis in the formation of NLCs is essentially complete. While ethanol, which is readily transported across lipid bilayers, was not expected to remain in the NLCs, the amount of Ca^{2+} remaining associated with the plasmid or inside the particles was not known. Determination of calcium ion concentration in DOPC NLCs after dissolution with Triton X-100 detergent and using Indo-1 as a sensor showed that $>99.8\%$ of the Ca^{2+} was removed in the dialysis procedure (data not shown). Given a trapped volume of roughly 5–10% for 150-nm liposomes at a 20 mM lipid concentration, it is clear that most of the calcium is removed before the integrity of the NLC membrane is established. The remaining calcium is at a concentration 300-fold lower than DNA phosphates on a mole basis, which is certainly insufficient to maintain any condensed structure.

Table 3
Surface potentials of SUVs and NLCs prepared with two lipid compositions

Lipids	Form	Zeta potential (mV)
DOPC	SUVs	−2.3 (6.4)
	NLCs[a]	−3.0 (6.4)
DOPC/DOPE(1:1)	SUVs	−10.7 (6.6)
	NLCs[b]	−9.5 (10.3)

[a]DOPC NLCs were prepared with 47.5% ethanol and 4 mM Ca^{2+}, effective diameter 133 nm, and trapping efficiency 69%.
[b]DOPC/DOPE NLCs were prepared with 40% EtOH and 5 mM Ca^{2+}, effective diameter 159 nm, and trapping efficiency 75%.

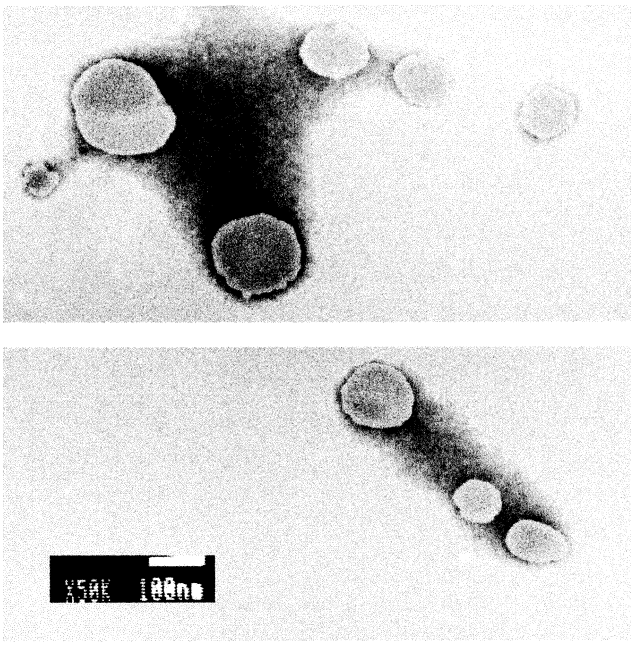

Fig. 2. Negative stain electron micrograph of NLCs formed with DOPC SUVs and pCMV-CAT plasmid, 48% ethanol (v/v) and 4.25 mM Ca^{2+}. The largest particle (upper left) appears to be an aggregate of two relatively large NLCs. Magnification, 27 000×, and the white bar of the inset indicates 100 nm.

Association of the plasmid with the fused liposomes in the NLCs was initially demonstrated by 1% agarose gel electrophoresis and by floatation on a 10% Ficoll gradient (data not shown). In both cases, the majority of the plasmid remained associated with the lipid. However, neither of these methods demonstrates that the plasmid is actually encapsulated in, and protected by, the lipid. Entrapment of plasmid measured by TO-PRO-1 binding confirms that the NLC membrane is indeed impermeable to small hydrophilic molecules. More importantly, it demonstrates that the plasmid is likely to be protected from degrading enzymes in vivo. It has been demonstrated previously [39] that inhibition of TO-PRO-1 binding is predictive of nuclease-mediated degradation. Indeed, this small-molecule probe can likely access DNA in structures that sterically exclude nucleases.

Further evidence that the fraction of plasmid protected from TO-PRO-1 binding is entrapped in the NLC particles, and not merely bound externally to the liposomes in a condensed form inaccessible to the

dye, comes from the surface potential measurements given in Table 3. Both DOPC and DOPC/DOPE (1:1) NLCs have zeta potentials identical to the SUVs from which they were prepared. The values indicate nearly neutral surfaces, with a slight negative charge contributed by deprotonated PE. For comparison, a typical cationic lipid–DNA complex particle has a zeta potential of about +50 mV [37].

The DOPC NLCs observed by negative stain electron microscopy, shown in Fig. 2, are consistent with the average particle size determined by light-scattering measurements. With this technique, liposomes appear as light globules surrounded by dark areas of uranyl acetate stain. Uncondensed DNA plasmids are not visible using this technique. As expected, the particles are not uniform in size. Calculated polydispersities from the autocorrelation function were typically 0.2–0.3. Yet, no particles with diameters greater than 250 nm were observed in any fields. Judging from the size and number of the smallest liposomes visualized, more than half of the liposomes undergo at least one fusion event, while the larger structures must have been formed from 5 to 10 SUVs. It is likely that the larger structures contain the most, if not all, of the entrapped plasmid (~60% trapping efficiency), but there are no discernible morphological differences between the large and small liposomes. The smooth continuous surfaces of most of the particles clearly indicate that the liposomes have indeed fused and are not merely aggregated.

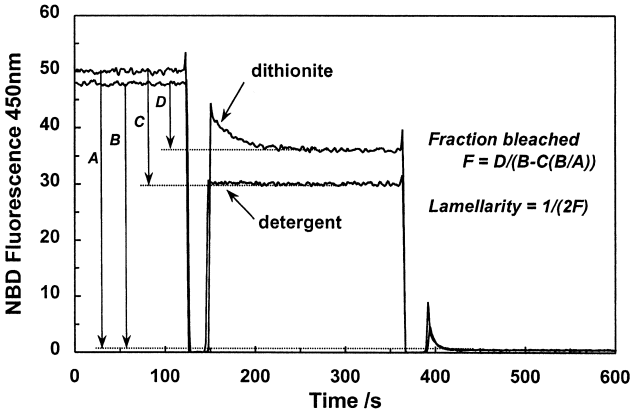

	Average Lamellarity	S.D.
SUVs	0.863	0.008
NLCs	1.220	0.011

Fig. 3. Determination of lamellarity for DOPC SUVs and NLCs by dithionite bleaching of NBD-DOPE. SUVs were prepared with 0.1 mol% NBD-DOPE in DOPC and were 77 ± 9 nm in diameter. NLCs formed with 47.5% ethanol and 4 mM Ca^{2+} were 150 ± 30 nm. Tabulated average lamellarities and standard deviations are derived from three measurements of a single DOPC NLC preparation.

The lamellarity of DOPC NLCs was determined by an NBD bleaching assay (Fig. 3). The method involves determining what fraction of the fluorescence of NBD-labeled lipid is rapidly lost upon the addition of the reducing agent, sodium dithionite. This fraction represents the fraction of lipid available to the bulk solution. Any remaining NBD fluorescence arises from lipids either on the inner leaflet of unilamellar vesicles or on all but the outermost leaflet of MLVs. Since the measured fluorescence of the NBD-DOPE is increased by scatter in the presence of liposomes, the fractional bleaching was corrected for this scatter by subtracting the loss of signal upon dispersing the liposomes with a non-ionic detergent. This correction may be obviated by the use of a low-pass cutoff filter.

The determined lamellarity value for the DOPC NLCs was 1.22 ± 0.01. This value indicates that the majority of the lipids are present as unilamellar vesicles. That the value is fractionally greater than one suggests that at least some of the resulting liposomes are bi- or multi-lamellar, or that some degree of aggregation is present. The lamellarity measured for DOPC SUVs (0.86 ± 0.01) is close to the expected value, since small liposomes of high curvature have a greater proportion of their lipids on the outer monolayer than the inner. For the NBD-DOPE containing SUVs (77 ± 9 nm diameter), measured lamellarity would be expected to be 0.89 ± 0.02, assuming an arbitrary constant headgroup area per lipid and a bilayer thickness of 4.0 nm.

DOPC and DOPC/DOPE (1:1) NLCs are physically stable for at least 2 weeks in PBS at 4°C. No changes in particle size or entrapment were found. Even at pH 4.0 or in the presence of 90% bovine serum for 1 h at 37°C these physical parameters remain unchanged (Fig. 4). The apparent minor decrease in size for the serum-treated samples actually arises from the light-scattering of serum particulates at the dilution of the measurement, as depicted in the serum-only control. No aggregation of NLCs or release of plasmid was detected. Stability was also demonstrated by concentrating the NLCs ten-fold

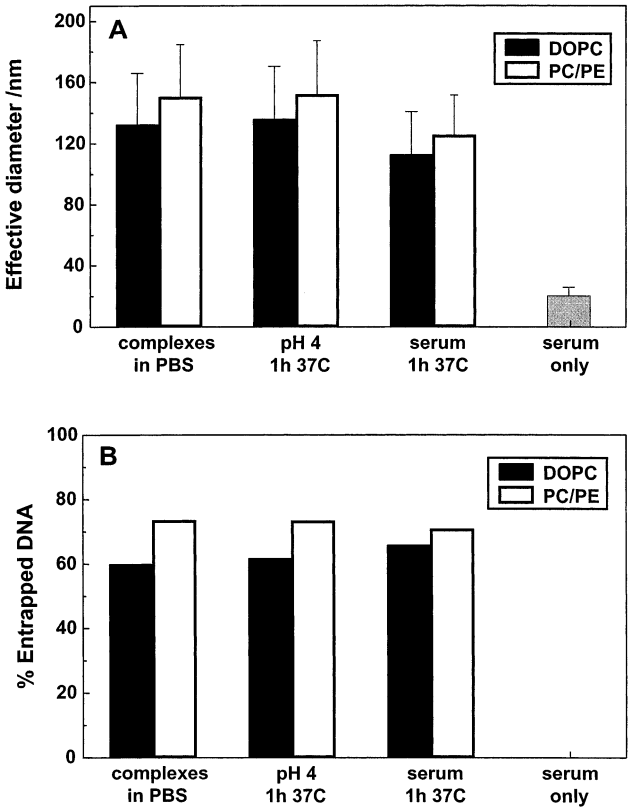

Fig. 4. Stability of DOPC and DOPC/DOPE (1:1) NLCs at pH 4.0 or in 90% fetal bovine serum for 1 h at 37°C. (A) Effective diameters from Gaussian fits to light-scattering autocorrelations with error bars indicating standard deviations of the fits. (B) Trapping efficiencies determined from the TO-PRO-1 assay.

(1.0 mg/ml DNA) by ultrafiltration using 100 K MWCO filters. Again, no change in size or entrapment was observed.

The in vivo circulation properties of DOPC NLCs were as expected for DOPC liposomes of the size measured. The distribution of NLC-associated lipid was determined following tail vein injection into mice using a radiolabeled lipid marker, and compared to SUVs (Fig. 5). After 1 h, about one-third of the injected lipid is still in circulation, both for the SUVs and the NLCs. This contrasts with cationic lipid–plasmid complexes that are cleared from the circulation within minutes [42]. The majority of the remaining recovered lipid is found in the liver and the spleen, as expected from previous reports with neutral liposomes [7]. A greater proportion of NLCs is found in these organs at 1 h than is observed for SUVs, and this is probably due to the larger particle size. Less than 2% of either SUVs or NLCs accumulated in the lungs, again in contrast to cationic lipid particles which accumulate substantially in the lungs following i.v. injection in tumor-bearing mice. Even less of the NLCs are found in the implanted SCC-VII tumors, which, although highly vascularized, may require longer times for significant accumulation of SUVs or complexes.

Only 25% of the injected plasmid DNA, as determined by qPCR, was recovered from the isolated tissues in these studies, compared to 60% of the lipid. Considering that only 60% of the plasmid was initially entrapped, about 10% of that initially entrapped DNA is no longer detectable in the tissues studies. Whether this difference reflects degradation of the plasmid, release of the plasmid from some of the liposomes in vivo, or differences in the recovery efficiencies of the assays is not known. However, for the plasmid that is detected, its distribution pattern is roughly the same as that of the lipid marker, suggesting that the DNA is still associated with and protected by the lipid. The highest amount of plasmid is in the circulation, clearly showing that it is protected from serum nucleases. The remainder is mainly distributed between the liver and the spleen in proportions corresponding to the amounts of lipid found in these organs. Less than 0.1% of the plasmid was found in either the lungs or the tumors. In tissues harvested at 18 h post-injection, only 0.05% total of the injected plasmid dose could be detected in all tissues analyzed (not shown).

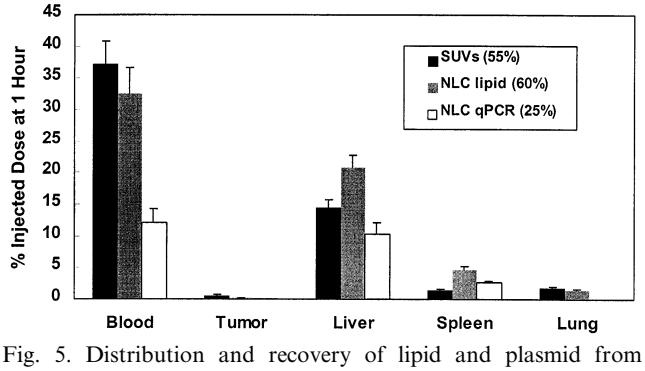

Fig. 5. Distribution and recovery of lipid and plasmid from DOPC NLCs 1 h following intravenous injection in mice. Lipid was tracked with radiolabeled cholesteryl hexadecyl ether, plasmid by quantitative PCR. The total fraction of the injected dose recovered is indicated in brackets. A control group injected with DOPC SUVs is also shown. Error bars indicate standard errors of the means with $n=5$.

4. Discussion

The entrapment of up to 80% of DNA plasmids inside stable, uncharged liposomes smaller on average than 200 nm in diameter is a two- to three-fold improvement over the best trapping efficiency previously reported for liposomes of this size. Most other techniques have given larger particles with considerably lower entrapment levels. The highly efficient trapping process described here takes advantage of several physical properties of plasmids, liposomes and their interactions with ethanol and calcium ions.

The physical properties of the NLCs clearly show that the plasmid DNA is entrapped inside liposomes formed through ethanol- and calcium-induced fusion of SUVs. Although it is conceivable that a very tight aggregation of SUVs with plasmid entrapped inside the aggregates could explain the lack of TO-PRO-1 binding and the lack of surface charge on the complexes, the electron microscopy, the lamellarity and all the stability results indicate a more robust structure. Furthermore, it is difficult to imagine what would provide the stable cohesive forces for such aggregates after the complete removal of calcium and ethanol. It may be possible to quantify the fusion process using existing lipid mixing assays [43,44], but the possibility of lipid probe transfer at the high ethanol concentrations used in the formation of the NLCs would make the interpretation of the results of such assays questionable.

Calcium ions are able to neutralize the phosphate charges of the DNA backbone, as well as to disrupt hydrogen bonding between base pairs. These processes are enhanced in the presence of ethanol, which both reduces the dielectric constant of the medium, to increase ionic interactions, and disorder the structured water around the native DNA. Ethanol alone can precipitate DNA by this dehydration process, promoting inter-helix association, but condensation is likely to be more efficient in the presence of Ca^{2+}, which can decrease inter-helical spacing and increase local bending through charge neutralization and base-pair disruption.

Zwitterionic liposomes are also affected in several ways by the presence of ethanol and calcium. Ethanol fluidizes PC vesicles, making them more permeable to hydrophilic solutes, but, more importantly, increasing their propensity to bend and permitting the formation of the non-bilayer intermediates that lead to fusion between vesicles [45]. This process probably involves disruption of the ordered water at membrane surface. Ethanol also fluidizes the bilayer by partitioning into the hydrocarbon region and increasing lipid headgroup spacing. For saturated phospholipids, ethanol can also induce interdigitation of monolayers, decreasing bilayer thickness.

The nature of interactions between calcium ions and a zwitterionic lipid surface is less clear. It is evident from Budker's work [29–31] that calcium promotes plasmid–lipid interactions in the absence of ethanol. This suggests that calcium is able to complex to some arrangement of the PC headgroups, possibly through a combination of ionic interactions with phosphates and electronic interactions with oxygen in the glycerol backbone. If this is so, the counterions of calcium must also be involved in the complex to maintain charge neutrality. Calcium has also been observed to promote fusion of DSPC/Chol liposomes to the plasma membrane of cells in vitro (Bailey and Chernomordik, unpublished). These observations suggest that calcium salts either create defects in lipid packing or promote curvature changes that can lead to membrane fusion.

The mechanism of NLC formation is clearly a complex process and probably involves several or all of these effects described above. Additionally, calcium may be forming salt bridges between liposomes and DNA to promote fusion and entrapment. In contrast to earlier reports for calcium-induced entrapment [29], it is clear from the electron microscopy and size analysis that fusion between liposomes is involved. Aggregation and fusion of liposomes, condensation of plasmid, and association of plasmid with liposomes must all be occurring simultaneously and interdependently. In the absence of plasmid, the extent of liposome fusion is much less, judged by particle size after dialysis. The dependence on calcium to achieve smaller particle sizes suggests that condensing or condensed plasmid can bridge and fuse fewer liposomes than uncondensed plasmid.

The choice of calcium over other divalent ions is important because of calcium's relatively weak ability to promote condensation. Attempts to entrap DNA in neutral liposomes with Mn^{2+} gave very large particles with limited trapping. Magnesium may behave more similarly to calcium, although it

is reported to have lower binding affinity. Also, the ethanol used in the entrapment process could probably be replaced by methanol or another miscible, dielectric-reducing solvent, but whether differences in either plasmid condensation or the liposome fusion induced would give comparable trapping efficiencies is not known.

The in vivo results clearly demonstrate the higher stability of neutral liposomes as a carrier for DNA plasmids compared to cationic lipid complexes. The circulation properties of NLCs are essentially the same as observed for empty liposomes, with about one-third of the complexes still circulating in the bloodstream after 1 h. While this clearance rate is still faster than that achieved with combinations of saturated PCs and cholesterol, it may be possible to extend the circulation times of NLCs by the incorporation of sterically stabilizing components, e.g. lipid-anchored polyethylene glycol (PEG), acyl glucoronides, or gangliosides [46]. However, the circulation properties of the NLCs as reported may be sufficient to achieve targeting to specific tissues using existing antibody, carbohydrate, or peptide targeting strategies [3].

The main concern is whether it will be possible to achieve transfection with NLCs upon delivery to cells. It was not expected that complexes made from these neutral lipids would be able to mediate release of entrapped plasmid from the endosomal compartment following uptake by cells, thereby preventing lysosomal degradation. NLCs were not affected by low pH or serum in vitro. The ability to achieve endosomal release is an important property of the cationic lipid complexes, although the mechanism of release and delivery to the nucleus with cationic lipids remain poorly understood. Indeed, initial in vitro studies indicate that NLCs are taken up in high copy number by several cell types, but little, if any, significant transfection is observed. The application of NLCs for systemic plasmid delivery may therefore also require the inclusion of an endosomolytic component, such as the low pH-triggered, membrane-destabilizing peptides or polymers.

Of course, as the number of components in the liposomes is increased, there is a risk that the plasmid trapping process will be negatively affected. This would almost certainly be the case for liposomes bearing sterically stabilizing PEG, which would have to be added after complex formation. However, short targeting or fusogenic peptides anchored to the liposomes may not impact on the trapping efficiency, or it may be possible to adjust the calcium and ethanol concentrations to maintain high plasmid entrapment. The effects of these components can be studied using the statistical design and modeling process described here.

The high level of plasmid entrapment achieved in the NLC process described, certainly warrants continued investigation into their use as gene delivery vehicles for systemic administration. The non-toxic nature of neutral liposomes and the longer circulation lifetimes of NLCs relative to other non-viral systems are clear advantages. If it is indeed possible to achieve tissue-specific targeting and to overcome the barriers to cytosolic and nuclear delivery with existing or future technologies, NLCs will offer an important alternative non-viral delivery system for gene therapy.

Acknowledgements

The authors would like to thank their colleagues and team members at Valentis, Inc., for technical support and advice in completing this work. In particular, we would like to acknowledge the efforts of Elizabeth Wilson, for the electron microscopy work, Khursheed Anwer and Ingrid Anscombe for the in vivo procedures, and Rosa Earls Johnson for the quantitative PCR results.

References

[1] K.L. Brigham, B. Meyrick, B. Christman, M. Magnuson, G. King, L.C.J. Berry, Am. J Med. Sci. 298 (1989) 278–281.
[2] B.D. Freimark, H.P. Blezinger, V.J. Florack, J.L. Nordstrom, S.D. Long, D.S. Deshpande, S. Nochumson, K.L. Petrak, J. Immunol. 160 (1998) 4580–4586.
[3] K. Anwer, A.L. Bailey, S.M. Sullivan, Critical Reviews in Therapeutic Drug Carrier Systems, in press.
[4] A. Gabizon, Ann. Biol. Clin. (Paris) 51 (1993) 811–813.
[5] P.G. Tardi, N.L. Boman, P.R. Cullis, J. Drug Target 4 (1996) 129–140.
[6] M. Gulati, S. Bajad, S. Singh, A.J. Ferdous, M. Singh, J. Microencapsul. 15 (1998) 137–151.
[7] M.J. Ostro, P.R. Cullis, Am. J. Hosp. Pharm. 46 (1989) 1576–1587.

[8] F.J. Szoka, D. Papahadjopoulos, Proc. Natl. Acad. Sci. USA 75 (1978) 4194–4198.
[9] R. Fraley, S. Subramani, P. Berg, D. Papahadjopoulos, J. Biol. Chem. 255 (1980) 10431–10435.
[10] N. Haga, K. Yagi, J. Clin. Biochem. Nutr. 7 (1989) 175–183.
[11] C.J. Kirby, G. Gregoriadis, J. Microencapsul. 1 (1984) 33–45.
[12] D.W. Deamer, G.L. Barchfeld, J. Mol. Evol. 18 (1982) 203–206.
[13] J. Xie, R. Peng, J. Chu, M. Wu, Prog. Nat. Sci. 3 (1993) 105–108.
[14] C.Y. Wang, L. Huang, Proc. Natl. Acad. Sci. USA 84 (1987) 7851–7855.
[15] S.E. Straus, T. Wilson, H.J. Raskas, J. Virol. 39 (1981) 290–294.
[16] L.D. Mayer, M.J. Hope, P.R. Cullis, Biochim. Biophys. Acta 858 (1986) 161–168.
[17] P.A. Monnard, T. Oberholzer, P. Luisi, Biochim. Biophys. Acta 1329 (1997) 39–50.
[18] D.M. Fishman, G.D. Patterson, Biopolymers 38 (1996) 535–552.
[19] R.W. Wilson, V.A. Bloomfield, Biochemistry 18 (1979) 2192–2196.
[20] J.H. van de Sande, L.P. McIntosh, T.M. Jovin, EMBO J. 1 (1982) 777–782.
[21] C. Ma, V.A. Bloomfield, Biophys. J. 67 (1994) 1678–1681.
[22] S. Kornilova, E. Hackl, L. Kapinos, V. Andrushchenko, Y. Blagoi, Acta Biochim. Pol. 45 (1998) 107–117.
[23] S. Flock, R. Labarbe, C. Houssier, Biophys. J. 71 (1996) 1519–1529.
[24] H. Votavova, D. Kucerova, J. Felsberg, J. Sponar, J. Biomol. Struct. Dyn. 4 (1986) 477–489.
[25] V.A. Bloomfield, Biopolymers 31 (1991) 1471–1481.
[26] Y. Fang, T.S. Spisz, J.H. Hoh, Nucleic Acids Res. 27 (1999) 1943–1949.
[27] K.B. Roy, T. Antony, A. Sakena, H.B. Bohidar, J. Phys. Chem. B 103 (1999) 5117–5121.
[28] Y. Blagoi, V.A. Sorokin, V.A. Valeev, G.O. Gladchenko, Biopolymers 22 (1983) 1641–1656.
[29] V.G. Budker, E.V. Kiseleva, A.V. Sokolov, Biol. Membr. 4 (1987) 1201–1208.
[30] V.G. Budker, A.V. Sokolov, Biol. Membr. 4 (1987) 639–647.
[31] V.G. Budker, A.V. Sokolov, L.M. Vainer, A.G. Krainev, Biol. Membr. 4 (1987) 55–66.
[32] M.R. Mozafari, V. Hasirci, J. Microencapsul. 15 (1998) 55–65.
[33] D.P. Kharakoz, R.S. Khusainova, A.V. Gorelov, K.A. Dawson, FEBS Lett. 446 (1999) 27–29.
[34] A.L. Bailey, P.R. Cullis, Biochemistry 36 (1997) 1628–1634.
[35] E.I. Pecheur, J. Sainte-Marie, A. Bienvenue, D. Hoekstra, Biochemistry 38 (1999) 364–373.
[36] Z. Chen, R.P. Rand, Biophys. J. 73 (1997) 267–276.
[37] R.I. Mahato, K. Anwer, F. Tagliaferri, C. Meaney, P. Leonard, M.S. Wadhwa, M. Logan, M. French, A. Rolland, Hum. Gene Ther. 9 (1998) 2083–2099.
[38] D.D. Steppan, J. Werner, R.P. Yeater, Essential Regression and Experimental Design. Internet publication, Gibsonia, PA, 1998.
[39] P. Harvie, F.M. Wong, M.B. Bally, Biophys. J. 75 (1998) 1040–1051.
[40] H.J. Gruber, H. Schindler, Biochim. Biophys. Acta 1189 (1994) 212–224.
[41] B.W. O'Malley Jr., K.A. Cope, C.S. Johnson, M.R. Schwartz, Arch Otolaryngol. Head Neck Surg. 123 (1997) 20–24.
[42] K. Anwer, P. Szymanski, G. Kao, Q. Ziang, R. Shelvin, S.M. Sullivan, Polym Prep. (Am. Chem. Soc., Div. Polym. Chem.) 40 (1999) 299–300.
[43] A.L. Bailey, P.R. Cullis, Biochemistry 33 (1994) 12573–12580.
[44] D.K. Struck, D. Hoekstra, R.E. Pagano, Biochemistry 20 (1981) 4093–4099.
[45] A. Chanturiya, E. Leikina, J. Zimmerberg, L.V. Chernomordik, Biophys. J. 77 (1999) 2035–2045.
[46] N. Oku, Y. Tokudome, H. Tsukada, T. Kosugi, Y. Namba, S. Okada, Biopharm. Drug Dispos. 17 (1996) 435–441.